4.2

Fatigue Crack Propagation under Mode I Conditions

B. Tomkins, J. Wareing and G. Sumner
UKAEA, Reactor Fuel Laboratories, Springfields, Preston, England

The process of fatigue failure in ductile metals is predominantly the steady controlled growth of a crack. In most situations, fatigue cracks propagate under mode I opening conditions. For small cracks in thick sections, stress conditions approximate to plane strain. True mode I growth produces a flat fracture surface perpendicular to the driving stress and for growth rates of 1-10 μm/cycle, the propagation process is one of sliding-off in the regions of maximum shear at the crack tip. For higher growth rates hole growth is involved in the crack extension process and potentially unstable conditions prevail. The result of the sliding-off process is a rippled fracture surface and for such growth, it has been found that often one ripple is formed on each successive cycle. It is important to realize that the same sliding-off process can operate at all levels of stress and strain. It therefore dominates the low cycle fatigue region as well as the low stress crack growth region. This would indicate that a unified law of crack growth can be formulated for both high and low strain crack propagation.

For plasticity controlled growth by sliding-off, a dependence of crack extension on the extent of the internal flow zone (D) ahead of the crack would be expected. At low stress levels this would be equal to the plastic zone size.

$$\frac{da}{dN} \propto D \propto \frac{\sigma^2 a}{T^2} \propto \frac{K^2}{T^2} \qquad (1)$$

where K is the stress intensity factor and T a representative flow stress for the zone. Such a growth rate dependence on K is known to hold for low stress crack growth in the ripple growth region. It has also been found by the authors to hold for the high strain region in a low alloy steel. For a more general law, one must determine the other parameters involved in the growth law. From the equation it can be seen that they are of non-dimensional form e.g. they have the dimensions of strain. The choice of other parameters depends on the choice of a realistic criteria for crack advance.

McClintock has suggested the crack tip displacement as a reasonable criteria for growth by sliding-off for low strain fatigue ($\Delta\epsilon_p = 0$), equation (1) then becomes, for $\frac{\sigma}{T} < 0.7$,

$$\frac{da}{dN} = \frac{CTOD}{2} = \alpha \frac{\Delta K^2}{ET} \qquad (2)$$

where α depends on the type of loading.

When some plastic straining is present, E would vary whilst T remains fairly constant and for a power law hardening material ($\Delta\sigma = k\Delta\epsilon_p^{\beta}$), the $CTOD$ must be integrated for increasing σ and equation (2) becomes,

$$\frac{da}{dN} = \frac{CTOD}{2} = \alpha\left[\frac{\Delta K^2}{ET} + \frac{4\pi\Delta\sigma\Delta\epsilon_p a}{T(1+\beta)}\right] \qquad (3)$$

In the high strain region ($\Delta\epsilon_p \gg \Delta\epsilon_e$), equation (3) shows a marked dependence of growth rate on $\Delta\epsilon_p$.

In figure 1, crack propagation data is presented for annealed En1A steel (mild steel) tested in push-pull loading. (In all tests, whose results are presented in this paper, crack growth is from a 50–250 μm spark machined starter edge notch in a 5.0 mm square section specimen). The data shows the strong dependence of growth rate on plastic strain range. The dashed curves show the variation

in ripple spacing taken from fractographic examination of the fracture surface. These curves are in agreement with equation (3). Hence the ripple spacing correlates well with $CTOD$. However, the crack growth rate is much less than this at the lower plastic strain amplitudes. This indicates a much stronger relative dependence of growth rate on plastic strain range than given by equation (3). The K^2 form of the curves is still generally correct, however.

For the high strain crack growth region, Tomkins has proposed that,

$$\frac{da}{dN} \propto \Delta\epsilon_p D \qquad (4)$$

the actual amount of new fracture surface being a proportion of the $CTOD$. Fig. 2 shows a plot of the function $K^2\Delta\epsilon_p$ vs $\frac{da}{dN}$ for the En1A steel and an austenitic stainless steel 20/25/Nb tested at room temperature and 750°C. The curves are in agreement with equation (4) and show a dependence on T^2 which equation (4) would predict.

However, equation (4) is obviously in error when $\Delta\epsilon_p \ll \Delta\epsilon_e$. In considering low alloy steels, Tomkins found that equation (4) was in error when cracking occurred in the plastic zone. The crack growth rate is then given by,

$$\frac{da}{dN} = (\Delta\epsilon_p + b\Delta\epsilon_e) D \qquad (5)$$

where $b \approx \frac{1}{6}$. Now some limiting strain condition can be expected in all materials over a finite region of the flow zone at the crack tip. Equation (5) would then be of general application with b a function of the ratio of flow strain to fracture strain (γ_u/γ_f).

Then equation (5) becomes,

$$\frac{da}{dN} = \left[\Delta\epsilon_p + b_1 \frac{\gamma_u}{\gamma_f} \Delta\epsilon_e\right] \qquad (5a)$$

For low strains ($\Delta\epsilon_p << \Delta\epsilon_e$),

$$\frac{da}{dN} = b_1\left(\frac{\gamma_u}{\gamma_f}\right)\frac{\Delta\sigma}{E}\frac{K^2}{T^2} \qquad (6)$$

Fig. 3 shows crack growth data for En25 (200) steel 2½% Ni-Cr-Mo steel; 200°C temper; true UTS = 1780 MN/m^2). The curves indicate a K^2 dependence and also an additional dependence on $\Delta\sigma$. It can be noted that the factor $(\gamma_u/\gamma_f).1/T^2$ means that the effect of T on crack growth is minimized at low stresses as observed by Barsom. Equation (5) offers a general crack propagation equation.

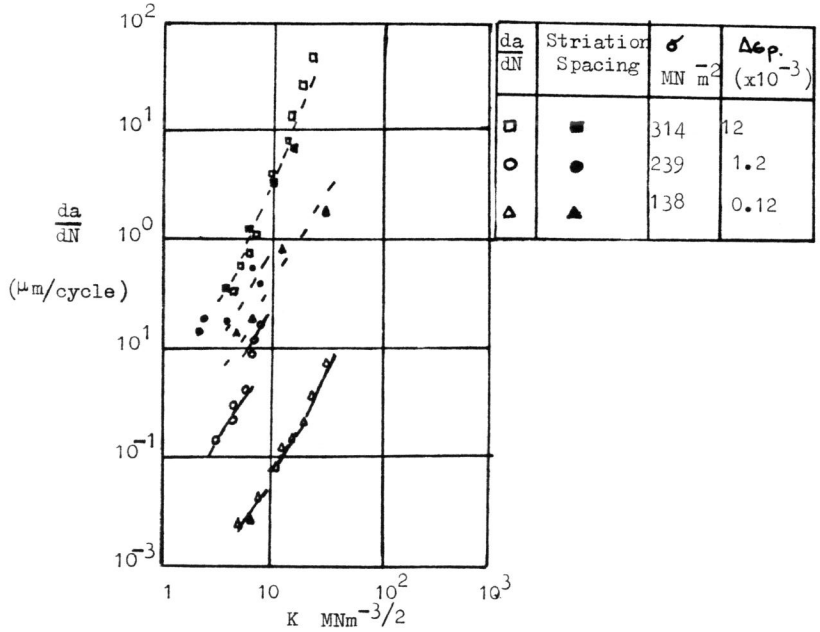

Fig 1 Dependence of crack growth rate and striation spacing on stress intensity factor EN1A steel at 25°C

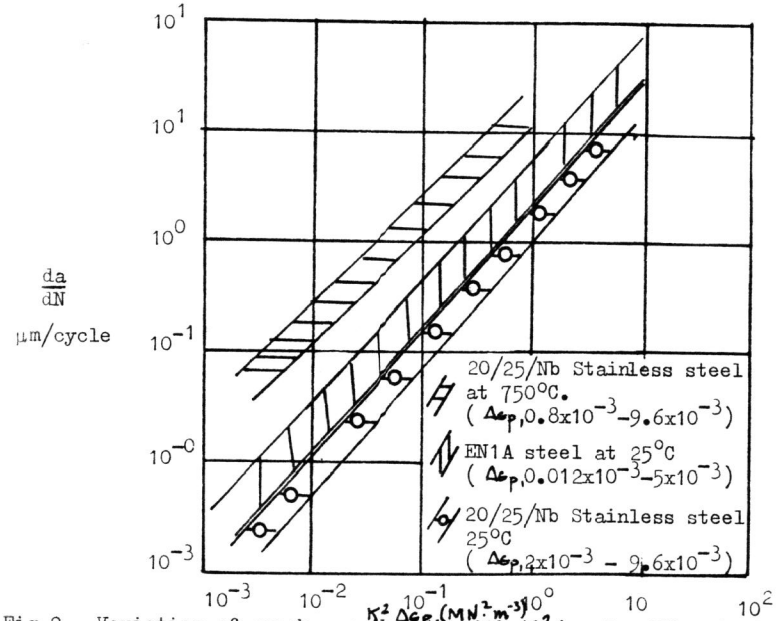

Fig 2 Variation of crack growth rate with $K^2\Delta\epsilon_p$ for EN1A steel and an austenitic stainless steel at 25°C and 750°C

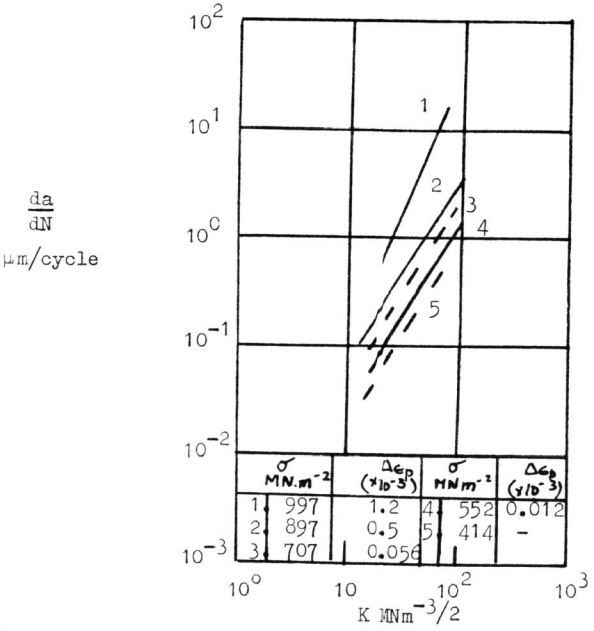

Fig 3 Variation of crack growth rate with stress Intensity Factor En 25(200) Steel at 25°C